J. Mater. Environ. Sci. 5 (6) (2015) 1519-1531
ISSN : 2028-2508
CODEN: JMESCN

Electrochemical study on the effectively of Hyoscyamus Muticus Extract as a green inhibitor for corrosion of copper in 1 MHNO_3

A.S. Fouda[1], Y.M. Abdallah[2,*], G.Y. Elawady[1], R.M. Ahmed[1]
[1] *Department of Chemistry, Faculty of Science, El-Mansoura University, El-Mansoura-35516, Egypt, Fax: +2 0502246254*
[2]*Faculty of Oral and Dental Medicine, Delta University for science and Technology, Gamasa, Egypt, Tel. +2 0502770140.*

Received 9August 2014, Revised 14 Jan 2015, Accepted 15 Jan 2015
[*] *Corresponding Author.E-mail: dr.ymostafa80@yahoo.com*

Abstract
Hyoscyamus Muticus Extract (HME), was investigated as a green corrosion inhibitor for copper in 1 M HNO_3 solution using weight loss, potentiodynamic polarization, electrochemical impedance spectroscopy (EIS) and electrochemical frequency modulation (EFM) techniques. Surface morphology was tested using scanning electron microscope (SEM). The effect of the temperature on corrosion behavior with addition of different concentrations was studied in the temperature range of 25-45 ºC by weight loss. Polarization curves reveal that the investigated extract is a cathodic behavior. The inhibition efficiency was found to increase with increase in the investigated extract concentration and decrease with increase in solution temperature. The adsorption of the inhibitor on copper surface was found to obey the Langmuir's adsorption isotherm. The activation and adsorption parameters were calculated and discussed. The results obtained from chemical and electrochemical techniques are in good agreement.

Keywords: Acidic inhibition, Copper, Hyoscyamus Muticus Extract, Green inhibitor, SEM.

Introduction
Corrosion is a fundamental process playing an important role in economics and safety, particularly for metals. The use of inhibitors is one of the most practical methods for protection against corrosion, especially in acidic media [1]. Most well-known acid inhibitors are organic compounds containing nitrogen , sulfur, and oxygen atoms. Among them, organic inhibitors have many advantages such as high inhibition efficiency and easy production [2-5].Organic heterocyclic compounds have been used for the corrosion inhibition of iron [6-9], copper [10], aluminum [11-13], and other metals [14-15] in different corroding media. Although many of these compounds have high inhibition efficiencies, several have undesirable side effects, even in very small concentrations, due to their toxicity to humans, deleterious environmental effects, and high-cost [16].
Plant extract is low-cost and environmental safe, so the main advantages of using plant extracts as corrosion inhibitor are economic and safe environment. Up till now, many plant extracts have been used as effective corrosion inhibitors for copper in acidic media, such as: Zenthoxylum alatum [17], Azadirachta Indica [18], caffeine [19] Cannabis [20]. The inhibition performance of plant extract is normally ascribed to the presence of complex organic species, including tannins, alkaloids and nitrogen bases, carbohydrates and proteins as well as hydrolysis products in their composition. These organic compounds usually contain polar functions with nitrogen, sulfur, or oxygen atoms and have triple or conjugated double bonds with aromatic rings in their molecular structures, which are the major adsorption centers.
Hyoscyamus Muticus, is a small genus of flowering plants in the nightshade family, Solanaceae. The eleven species it contains are known generally as the henbanes, is widely distributed in Mediterranean, The whole plant has great medicinal importance, as a poultice to relieve pain, The variation in alkaloid content by growth stage and among populations may be reasons for variations in its toxicity and its value as fodder [21].
The present work was designed to study the inhibitory action of Hyoscyamus Muticusfor the corrosion of copper in 1 M HNO_3 using weight loss, potentiodynamic polarization measurements, electrochemical impedance spectroscopy (EIS) measurements, electrochemical frequency modulation (EFM) technique, and Surface morphology was tested using scanning electron microscope (SEM).

2. Experimental Methods

2.1. Materials and Solutions

Experiments were performed using Copper specimens (99.98%) were mounted in Teflon. An epoxy resin was used to fill the space between Teflon and copper electrode. The auxiliary electrode was a platinum wire (1 cm^2), while a saturated calomel electrode (SCE) connected to a conventional electrolytic cell of capacity 100 ml via a bridge with a Luggin capillary, the tip of which was very close to the surface of the working electrode to minimize the IR drop. The aggressive solution used was prepared by dilution of analytical reagent grade 70% HNO_3 with bidistilled water. The stock solution (1000 ppm) of HME was used to prepare the desired concentrations by dilution with bidistilled water. The concentration range of HME used was 50-500 ppm.

2.2. Preparation of plant extracts

Fresh aerial parts of HME sample were crushed to make fine powder. The powdered materials (250 g) were soaked in 500 ml of dichloromethane for 5 days and then subjected to repeated extraction with 5× 50 ml until exhaustion of plant materials. The extracts obtained were then concentrated under reduced pressure using rotary evaporator at temperature below 50°C. The dichloromethane evaporated to give solid extract that was prepared for application as corrosion inhibitor.

Chemical studies have demonstrated that the HME contain many alkaloids as Hyoscine, Atropine and Hyoscyanine as the major compounds [22].

2.3. Weight lose measurements

Seven parallel copper sheets of 1×1×0.4 cm were abraded with emery paper (grade 320–500–1200) and then washed with bidistilled water and acetone. After accurate weighing, the specimens were immersed in a 250 ml beaker, which contained 100 ml of $HNO_3$with and without addition of different concentrations of HME.

All the aggressive acid solutions were open to air. After 180 minutes, the specimens were taken out, washed, dried, and weighed accurately. The average weight loss of seven parallel copper sheets could be obtained. The inhibition efficiency (IE%) and the degree of surface coverage, θ of HME for the corrosion of copper were calculated as follows [23],

$$IE\% = \theta \times 100 = \left[1 - \frac{W}{W^{\circ}}\right] \times 100 \quad (1)$$

where W^o and W are the values of the average weight loss without and with addition of the inhibitor, respectively.

2.4. Electrochemical measurements

Electrochemical measurements were performed using a typical three-compartment glass cell consisting of the copper specimen as working electrode (1 cm^2), saturated calomel electrode (SCE) as a reference electrode, and a platinum wire as a counter electrode. The reference electrode was connected to a Luggin capillary and the tip of the Luggin capillary is made very close to the surface of the working electrode to minimize IR drop. All the measurements were done in solutions open to atmosphere under unstirred conditions. All potential values were reported versus SCE. Prior to each experiment, the electrode was abraded with successive different grades of emery paper, degreased with acetone, also washed with bidistilled water, and finally dried.Tafel polarization curves were obtained by changing the electrode potential automatically from (-0.8 to 1 V vs. SCE) at open circuit potential with a scan rate of 1 mVs^{-1}. Stern-Geary method [24], used for the determination of corrosion current is performed by extrapolation of anodic and cathodic Tafel lines to a point which gives (log i_{corr}) and the corresponding corrosion potential (E_{corr}) for inhibitor free acid and for each concentration of inhibitor. Then (i_{corr}) was used for calculation of inhibition efficiency (IE %) and surface coverage (θ) as in equation 2:

$$IE\ \% = \Theta \times 100 = \left[1 - \frac{i_{corr\ (inh)}}{\mathrm{i}corr_{\ (free\ )}}\right] \times 100 \qquad (2)$$

where $i_{corr(free)}$ and $i_{corr(inh)}$ are the corrosion current densities in the absence and presence of inhibitor, respectively .

Impedance measurements were carried out in frequency range ($2x10^4$ Hz to $8x10^{-2}$ Hz) with amplitude of 10 mV peak-to-peak using ac signals at open circuit potential. The experimental impedance was analyzed and interpreted based on the equivalent circuit. The main parameters deduced from the analysis of Nyquist diagram are the charge transfer resistance R_{ct} (diameter of high-frequency loop) and the double layer capacity C_{dl}. The inhibition efficiencies and the surface coverage (θ) obtained from the impedance measurements are calculated from equation 3:

$$IE\% = \theta \times 100 = \left[1 - \left(\frac{R^{\circ}_{ct}}{R_{ct}}\right)\right] \times 100 \qquad (3)$$

where R^{o}_{ct} and R_{ct} are the charge transfer resistance in the absence and presence of inhibitor, respectively.
Electrochemical frequency modulation, EFM, was carried out using two frequencies 2 and 5 Hz. The base frequency was 0.1 Hz, so the waveform repeats after 1 s. The higher frequency must be at least two times the lower one. The higher frequency must also be sufficiently slow that the charging of the double layer does not contribute to the current response. Often, 10 Hz is a reasonable limit. The Intermodulation spectra contain current responses assigned for harmonical and intermodulation current peaks. The large peaks were used to calculate the corrosion current density (i_{corr}), the Tafel slopes (β_a and β_c) and the causality factors CF-2 & CF-3 [25]. The electrode potential was allowed to stabilize 30 min before starting the measurements. All the experiments were conducted at 25°C .
All electrochemical measurements were performed using Gamry Instrument (PCI4/750) Potentiostat/Galvanostat/ZRA. This includes a Gamry framework system based on the ESA 400. Gamry applications include DC105 software for potentiodynamic polarization, EIS 300 software for electrochemical impedance spectroscopy, and EFM 140 software for electrochemical frequency modulation measurements via computer for collecting data. Echem Analyst 6.03 software was used for plotting, graphing, and fitting data.
To test the reliability and reproducibility of the measurements, duplicate experiments, which performed in each case at the same conditions.

2.5. Surface morphology

For morphological study, surface features (1 cm x 1 cm x 0.4cm) of copper were examined before and after exposure to 1 M HNO_3 solutions for 4 hour with and without inhibitor. JEOL JSM-5500 scanning electron microscope was used for this investigation.

3. ResultsandDiscussion

3.1. Weight loss measurements

Weight loss measurements were carried out for copper in 1 M HNO_3 in the absence and presence of different concentrations of HME and are shown in Figure (1). The inhibition efficiency (IE%) values calculated are listed in Table 1, 2. From these tables, it is noted that the IE% increases steadily with increasing the concentration of HME and decrease with temperature rising from 25-45ºC. The inhibition efficiency (IE%) and surface coverage (θ)were calculated by equation (1).

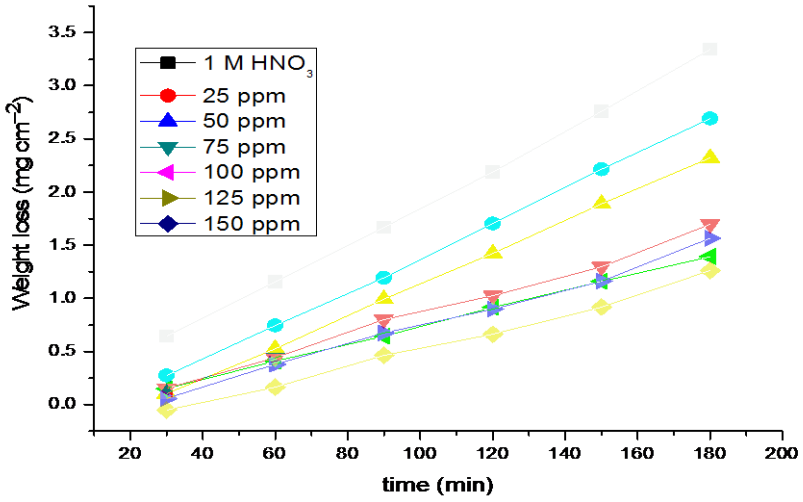

Figure1: Weight loss-time curves for the corrosion of copper in 1 M HNO_3in the absence and presence of different concentrations of HME at 25°C.

Table 1: Corrosion rate (C.R.) in (mg cm^{-2} min^{-1}) and inhibition efficiency data obtained from weight loss measurements for copper in 1 M HNO_3 solutions without and with various concentrations of HME at 25°C.

Conc., ppm	Weight loss, mg/cm^2	C.R., mg cm^{-2} min^{-1}	θ	%IE
1 M HNO_3	3.445	0.078	---	---
50 ppm	1.965	0.024	0.430	43.0
100 ppm	0.986	0.009	0.714	71.4
200 ppm	0.742	0.005	0.785	78.5
300 ppm	0.538	0.004	0.844	84.4
400 ppm	0.441	0.003	0.872	87.2
500 ppm	0.329	0.001	0.90	90.45

Table 2: Data of weight loss measurements for copper in 1 M HNO_3 solution in the absence and presence of different concentrations of HME at 25–45°C.

Conc., ppm	Temp., °C	C.R., $mgcm^{-2}min^{-1}$	θ	IE%
50	25	0.024	0.430	43.0
	30	0.075	0.416	41.6
	35	0.083	0.243	24.3
	40	0.120	0.211	21.1
	45	0.237	0.147	14.7
100	25	0.009	0.714	71.4
	30	0.015	0.520	52.0
	35	0.032	0.342	34.2
	40	0.056	0.217	21.7
	45	0.067	0.117	11.7
200	25	0.005	0.785	78.5
	30	0.014	0.677	67.7
	35	0.023	0.555	55.5
	40	0.040	0.486	48.6
	45	0.060	0.334	33.4
300	25	0.004	0.844	84.4
	30	0.011	0.729	72.9
	35	0.021	0.598	59.8
	40	0.032	0.603	60.3
	45	0.051	0.435	43.5
400	25	0.003	0.872	87.2
	30	0.010	0.761	76.1
	35	0.018	0.652	65.2
	40	0.028	0.650	65.0
	45	0.044	0.510	51.0
500	25	0.001	0.904	90.4
	30	0.008	0.806	80.6
	35	0.014	0.734	73.4
	40	0.024	0.699	69.9
	45	0.037	0.591	59.1

The observed inhibition action of the HME could be attributed to the adsorption of its components on copper surface. The formed layer, of the adsorbed molecules, isolates the metal surface from the aggressive medium which limits the dissolution of the latter by blocking of their corrosion sites and hence decreasing the corrosion rate, with increasing efficiency as their concentrations increase [26].

3.2. Polarization curves

Figure 2 shows potentiodynamic polarization curves recorded for copper in 1 M HNO_3 solutions in the absence and presence of various concentrations of HME at 25ºC.

Lee and Nobe [27] reported the occurrence of a current peak between the apparent-Tafel and limiting-current regions during potential sweep experiments.

The presence of HME shifts both anodic and cathodic branches to the lower values of corrosion current densities and thus causes a remarkable decrease in the corrosion rate. The parameters derived from the polarization curves in Figure 2 are given in Table 3. In 1 M HNO_3 solution, the presence of HME causes a remarkable decrease in the corrosion rate i.e., shifts both anodic and cathodic curves to lower current densities. In other words, both cathodic and anodic reactions of copper electrode are retarded by HME in 1 M HNO_3 solution. The Tafel slopes of β_a and β_c at 25ºCdo not change remarkably upon addition of HME, which indicates that the presence of HME does not change the mechanism of hydrogen evolution and the metal dissolution process. Generally, an inhibitor can be classified as cathodic type if the shift of corrosion potential in the presence of the inhibitor is more than 85 mV with respect to that in the absence of the inhibitor [28, 29]. In the presence of HME, E_{corr} shifts to less negative but this shift is very small (about 20-30 mV), which indicates that HME can be arranged as cathodic inhibitor.

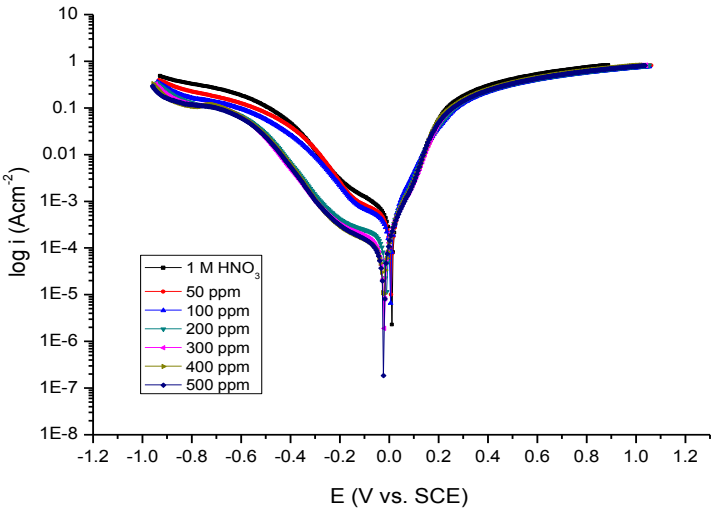

Figure 2: Potentiodynamic polarization curves for the corrosion of copper in 1 M HNO_3solution without and with various concentrations of HME at 25˚C.

Table 3: Effect of concentration of HME on the electrochemical parameters calculated using potentiodynamic polarization technique for the corrosion of copper in 1 M HNO_3 at 25˚C.

Concentration, ppm	i_{corr}, µA cm^{-2}	-E_{corr}, mV vs. SCE	β_a, mVdec^{-1}	β_c, mVdec^{-1}	CR, mm y^{-1}	θ	η %
1 M HNO_3	423.0	6.662	64.50	172.5	102.47	--	--
50	262.0	8.870	87.00	192.4	79.40	0.381	38.1
100	158.0	6.170	83.20	206.5	56.50	0.626	62.6
200	79.80	13.70	72.00	218.5	39.38	0.811	81.1
300	53.90	21.40	72.00	201.7	26.61	0.873	87.3
400	50.80	23.90	69.30	195.7	25.06	0.880	88.0
500	48.00	23.20	68.90	192.8	23.67	0.89	88.65

3.3. Electrochemical impedance spectroscopy (EIS)

Figure (3) shows impedance plots for copper in 1 M HNO_3 solution without and with different concentrations of HME extract. The impedance spectra consists of a Nyquist semicircle type without appearance of diffusive contribution to the total impedance (Z) indicating that the corrosion proceeds mainly under charge-transfer control and the presence of inhibitor do not alter the mechanism of corrosion reaction.

It is found that the obtained Nyquist plots are not perfect semicircle due to frequency dispersion and this behavior can be attributed to roughness and in homogeneities of the electrode surface [30, 31].
When there is non-ideal frequency response, it is common practice to use distributed circuit elements in an equivalent circuit. The most widely employed is the constant phase element (CPE). In general a CPE is used in a model in place of a capacitor to compensate for inhomogeneity in the system [32]. It was found that the diameters of the semicircle increases with increasing the concentration of the investigated extract. This indicates that the polarization resistance of the oxide layer increases with increasing the concentration of HME and the depressed capacitive semicircle are often referred to the surface roughness and inhomogeneity, since this capacitive semicircle is correlated with dielectric properties and thickness of the barrier oxide film [33]. The data revealed that, each impedance diagram consists of a large capacitive loop with low frequencies dispersion (inductive arc). This inductive arc is generally attributed to anodic adsorbed intermediates controlling the anodic process [34-36]. By following this, inductive arc was disregarded.

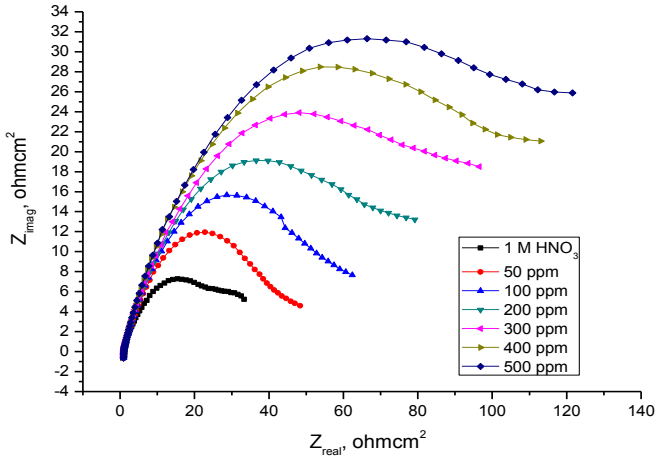

Figure 3: Nyquist plots for copper in 1 M HNO_3 solutions in the absence and presence of various concentrations of HME at 25°C.

The electrical equivalent circuit model shown in Figure (4) was used to analyze the obtained impedance data. The model consists of the solution resistance (R_s), the charge-transfer resistance of the interfacial corrosion reaction (R_{ct}) and the constant phase angle element (CPE). The value of frequency power (n) of CPE can be assumed to correspond to capacitive behavior. However, excellent fit with this model was obtained with our experimental data. The admittance of CPE is described as:

$$Y_{CPE} = Y_o(j\omega)^n \qquad (4)$$

where j is the imaginary root, ω the angular frequency, Y_o the magnitude and *n* the exponential term [37].

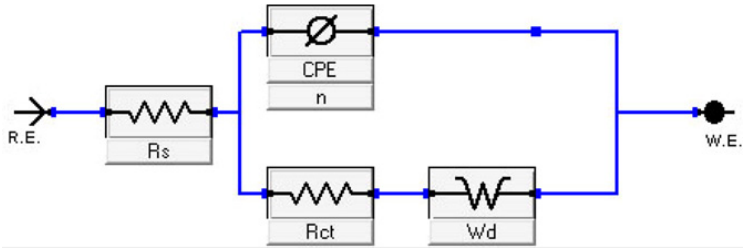

Figure 4: Equivalent circuit used to model impedance data for copper in 1 M HNO_3solutions.

A long Warburg diffusion tail was observed at low frequency values. The tails are inclined at an angle of 45° to the real-axis at the very low frequencies; A diffusion controlled process is therefore exists. Studies reported in the literature [38] showed that the diffusion process is controlled by diffusion of dissolved oxygen from the bulk solution to the electrode surface and the Warburg impedance, which is observed in the low frequency regions, is ascribed to diffusion of oxygen to the alloy surface. This diffusion tail still appears, even in presence of high

concentrations of the investigated extract. This means that the corrosion behavior of alloy in the absence as well as in the presence of HME is influenced by mass transport.
Also, Bode plots for the copper in 1 M HNO_3 solution are shown in Figure (5). In which the high frequency limit corresponding to the electrolyte resistance (ohmic resistance) R_Ω, while the low frequency represents the sum of (R_Ω + R_{ct}), where R_{ct} is in the first approximation determined by both electrolytic conductance of the oxide film and the polarization resistance of the dissolution and repassivation process. At both low and high frequency limits, the phase angle between the current and potential (θ), assumes a value of about 0°, corresponding to the resistive behavior of R_Ω and (R_Ω + R_{ct}).

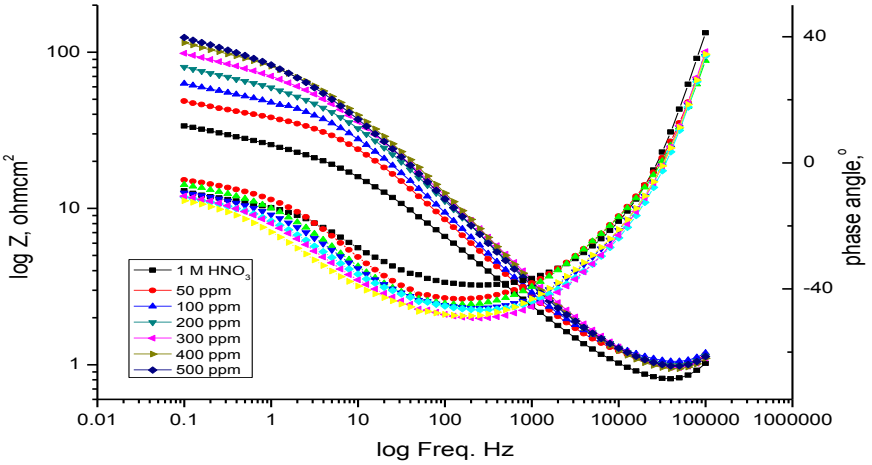

Figure 5: Bode plots for copper in 1M HNO_3 solutions in the absence and presence of various HME concentrations at 25°C

The main parameters deduced from the analysis of Nyquist diagram are:

- The resistance of charge transfer R_{ct}(diameter of high frequency loop)
- The capacity of double layer C_{dl} which is defined as :

$$C_{dl} = \frac{1}{2\pi R_{ct} f_{max}} \qquad (5)$$

where f_{max} is the maximum frequency at which the Z_{imag} of the impedance is a maximum. Since the electrochemical theory assumed that ($1/R_{ct}$) is directly proportional to the capacity of double layer C_{dl}, the inhibition efficiency (%IE) of the inhibitor for copper in 1 M HNO_3 solution was calculated from R_{ct} values obtained from impedance data at different inhibitor concentration the following equation:

$$\% IE = \left(1 - \frac{R^{\circ}_{ct}}{R_{ct}}\right) \times 100 \qquad (6)$$

where R^{o}_{ct} and R_{ct} are the charge transfer resistance in the absence and Presence of investigated extract, respectively.
From the impedance data given in Table (4), we can conclude that the value of R_{ct} increases with the increase in the concentration of the investigated extract and this indicates the formation of a protective film on the alloy surface by the adsorption and an increase in the corrosion inhibition efficiency in acidic solution. While the value of C_{dl} decreases with increasing the concentrations of extract in comparison with that of blank solution (uninhibited), as a result from the replacement of water molecules by inhibitor molecules which lead to decrease in local dielectric constant and/or an increase in the thickness of the electric double layer formed on the metal surface [39,40].

3.4. Electrochemical frequency modulation (EFM)
EFM is a nondestructive corrosion measurement technique that can directly determine the corrosion current value without prior knowledge of Tafel slopes, and with only a small polarizing signal. These advantages of EFM technique make it an ideal candidate for online corrosion monitoring [41]. The great strength of the EFM is the causality factors which serve as an internal check on the validity of EFM measurement. The causality factors CF-2 and CF-3 are calculated from the frequency spectrum of the current responses.

Table 4: Parameters obtained by fitting the Niquist plots shown in Fig. 3 with the equivalent circuit in Fig. 5 for copper in 1 M HNO_3 solutions in the absence and presence of various concentrations of HME at 25°C.

Concentration, ppm.	R_{ct}, Ωcm^2	Y_o	N	C_{dl}, $x10^4$ $\mu F\ cm^{-2}$	W, $\mu\Omega^{-1}cm^{-2}s^{1/2}$	θ	% IE
1 M HNO3	190.4	2.27E+01	4.7900	9.77E+00	3.75E+01	---	---
50	338.2	1.55E+01	3.2150	6.89E+00	6.32E+01	0.437	43.7
100	387.1	1.39E+01	2.8860	6.97E+00	4.97E+01	0.508	50.8
200	464.1	1.48E+01	3.0140	8.03E+00	3.71E+01	0.590	59.0
300	641.7	1.45E+01	2.9770	8.88E+00	3.53E+01	0.703	70.3
400	777.7	1.42E+01	2.8470	8.98E+00	3.67E+01	0.755	75.5
500	1023.0	1.32E+01	2.7560	9.66E+00	3.74E+01	0.814	81.4

Fig. 6 show the frequency spectrum of the current response of pure copper in 1 M HNO_3 solution, contains not only the input frequencies, but also contains frequency components which are the sum, difference, and multiples of the two input frequencies. The EFM intermodulation spectrums of Cu in 1 M HNO_3 solution containing (50ppm- 500ppm) of the HME extract at 25°C is shown in Fig. 6.

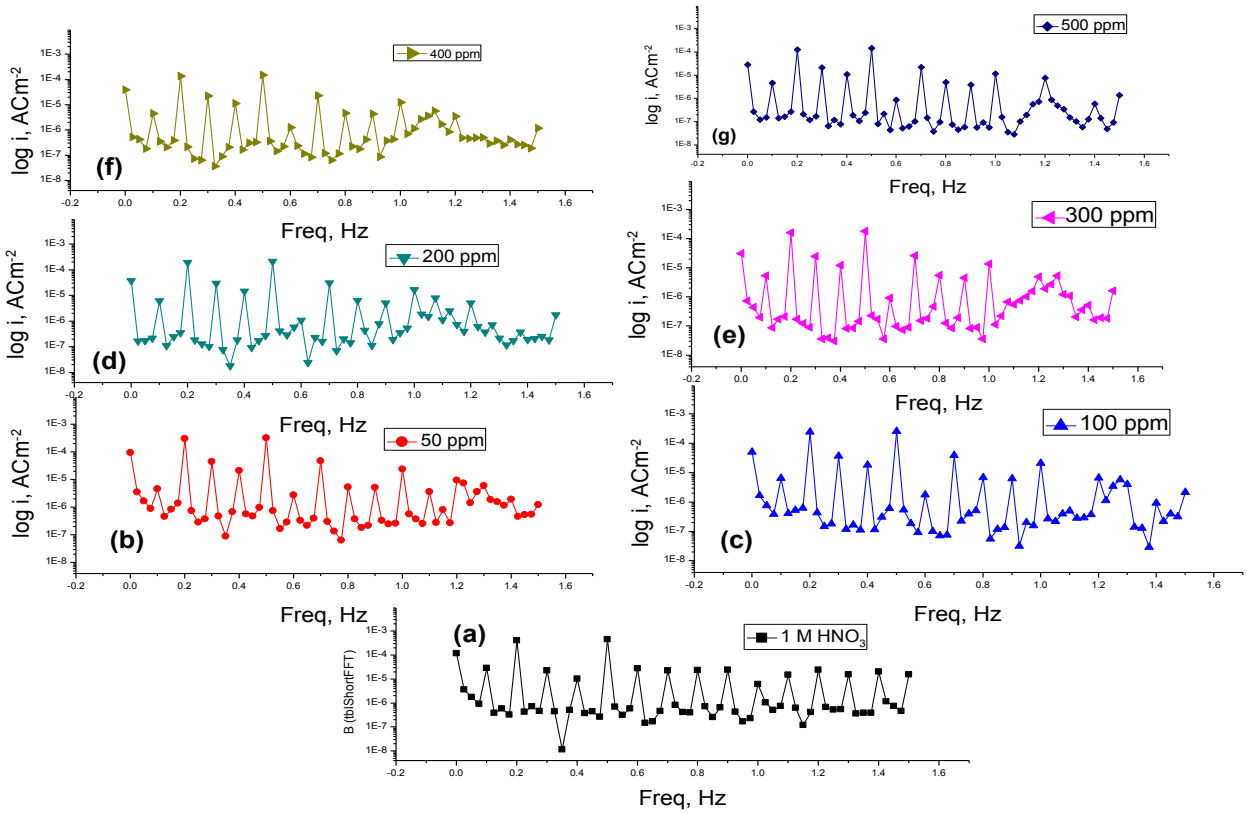

Figure 6 (a-g): Intermodulation spectrums for the corrosion of copper in 1 M HNO_3without and with various concentrations of HME at 25°C

The harmonic and intermodulation peaks are clearly visible and are much larger than the background noise. The two large peaks, with amplitude of about 200 µA, are the response to the 40 and 100 mHz (2 and 5 Hz) excitation frequencies. It is important to note that between the peaks there is nearly no current response (<100 mA). The experimental EFM data were treated using two different models: complete diffusion control of the cathodic reaction and the "activation" model. For the latter, a set of three non-linear equations had been solved, assuming that the corrosion potential does not change due to the polarization of the working electrode [42].The larger peaks were used to calculate the corrosion current density (i_{corr}), the Tafel slopes (β_c and β_a) and the causality factors

(CF-2 and CF-3).These electrochemical parameters were simultaneously determined by Gamry EFM140 software, and listed in Table 5 indicating that this extract inhibit the corrosion of copper in 1 M HNO_3 through adsorption. The causality factors obtained under different experimental conditions are approximately equal to the theoretical values (2 and 3) indicating that the measured data are verified and of goodquality [43]. The inhibition efficiencies IE_{EFM} % increase by increasing the studied extract concentrations and was calculated as follows:

$$IE\ \%_{EFM} = \left(1 - \frac{i_{corr}}{i^{o}_{corr}}\right) \times 100 \qquad (7)$$

where i^{o}_{corr} and i_{corr} are corrosion current densities in the absence and presence of HME extract, respectively.

Table 5: Electrochemical kinetic parameters obtained by EFM technique for Cu in1 M HNO_3 solutions containing various concentrations of HME at 25°C.

Concentration, ppm	i_{corr}, µA	β_a mV dec^{-1}	β_c mV dec^{-1}	C.R. mpy	CF-2	CF-3	θ	%IE
1 M HNO_3	527.6	44.80	52.41	157.7	1.88	2.81	---	---
50	261.9	72.67	70	123.5	2.05	3.04	0.504	50.4
100	206.9	61.78	80	119.88	1.96	3.34	0.608	60.8
200	181.9	60.07	133.9	93.02	1.93	3.12	0.655	65.5
300	141.1	57.98	122	75.88	1.94	3.09	0.733	73.3
400	123.4	58.53	83	56.22	1.92	3.46	0.766	76.6
500	87.5	50.59	100.1	43.88	1.92	3.48	0.834	83.4

3.5. Adsorption Isotherm

The mode and interaction degree between an inhibitor and a metallic surface have been widely studied with the application of adsorption isotherms. The adsorption of an organic molecule occurs because the interaction energy between an inhibitor and a metallic surface is higher than that between water molecules and metallic surface [44, 45]. To obtain the adsorption isotherms, the degree of surface coverage (θ) obtained from weight loss method was determined as a function of inhibitor concentration. The values of θ were then plotted to fit the most suitable model of adsorption [46].Attempts were made to fit experimental data to various isotherms including Frumkin, Langmuir, Temkin, Freundlich, isotherms. By far the results were best fitted by Langmuir adsorptionisotherm as seen in Figure 7 [47]:

$$\frac{C}{\theta} = \frac{1}{K} + C \qquad (8)$$

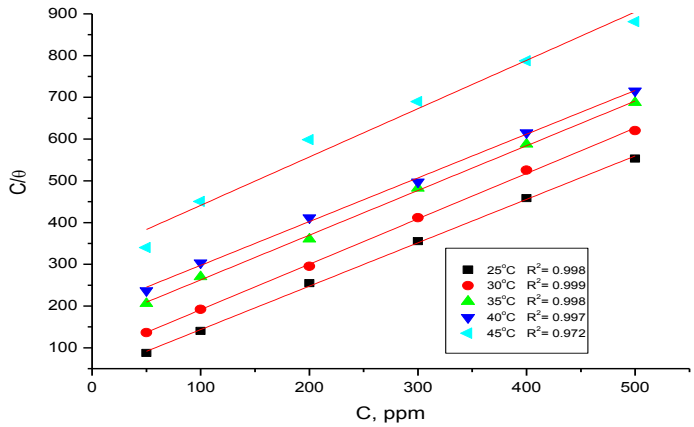

Figure 7: Langmuir adsorption plots for copper in 1 M HNO_3 containing various concentrations of HME at 25°C.

3.6. Kinetic-thermodynamic corrosion parameters

Weight loss method was carried out at different temperature (25°C–45°C) in the presence of different concentration of HME. It has been found that he corrosion rate increases with the increase in temperature for HME (Table 2). The corrosion rate of copper in the absence of HME increased steeply from 25 to 45°Cwhereas;

in the presence of HME the corrosion rate decreased slowly. The inhibition efficiency was found to decrease with temperature. The corrosion parameter in the absence and presence of extract in the temperature range 25–45°C has been summarized in Table 2.The apparent activation energy (E^*_a) for dissolution of copper in 1M HNO_3 was calculated from the slope of plots by using Arrhenius equation:

$$\log k = \frac{-E_a^*}{2.303\ R\ T} + \log A \qquad (9)$$

where k is rate of corrosion, E^*_a is the apparent activation energy is the universal gas constant, T is absolute temperature and A is the Arrhenius pre-exponential factor.

By plotting log k against 1/T the values of activation energy (E^*_a) has been calculated (E^*_a = (slope) 2.303 x R) (Fig. 8). Activation energy for the reaction of copper in 1M HNO_3increases in the presence of extract (Table6). This increasing in activation energy E^*_aindicates the formation of chemical bonds were strengthen by increasing the temperature. However, the extent of the rate increment in the inhibited solution is higher than that in the free acid solution. Therefore, the inhibition efficiency of the HMEdecreasesmarkedly with increasing temperature. This result supports the idea that the adsorption of extract components on the copper surface may be chemical in nature. Thus, as the temperature increases the number of adsorbed molecules increases leading to an increase in the inhibition efficiency. The obtained results suggest that HME inhibits the corrosion reaction by increasingits activation energy. This could be done by adsorption on the copper surface making a barrier for mass and charge transfer. However, such types of inhibitors perform a good inhibition at high temperature with considerable increase in inhibition efficiency at elevated temperatures [48]. Moreover, the relatively low value of activation energy in presence of HME suggests a physical adsorption process.

The values of change of entropy (ΔS^*) and change of enthalpy (ΔH^*) can be calculated by using the formula:

$$k = \left(\frac{RT}{Nh}\right) exp\left(\frac{\Delta S^*}{R}\right) exp\left(\frac{\Delta H^*}{RT}\right) \qquad (10)$$

where k is rate of corrosion, h is Planck's constant, N is Avogadro number, ΔS^* is the entropy of activation, and ΔH^* is the enthalpy of activation. A plot of log (k/T) vs. 1/T (Fig. 9) should give a straight line, with a slope of (ΔH^*/2.303R) and an intercept of [log (R/Nh)+ΔS^*/2.303R], from which the values of ΔS^* and ΔH^* can be calculated (Table 6).The negative value of ΔS^* for the inhibitor indicates that activated complex in the rate determining step represents an association rather than a dissociation step, meaning that a decrease in disorder takes place during the course of transition from reactant to the activated complex [49] The negative sign of ΔH^* indicates that the adsorption of inhibitor molecules is an exothermic process. Generally, an exothermic process signifies either physisorption, chemisorption's or a combination of both.

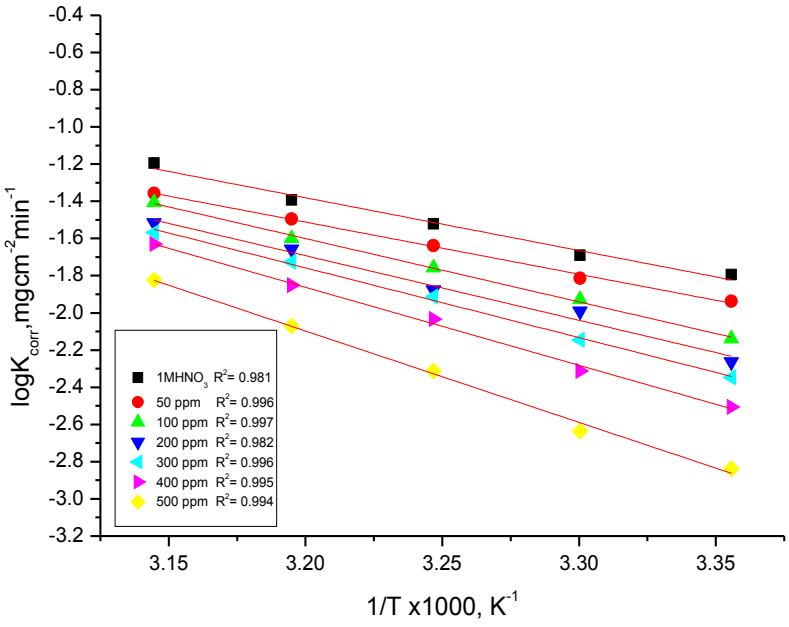

Figure 8: log k (corrosion rate) – 1/T curves for copper in 1 M HNO_3 in the absence and presence of different concentrations of HME.

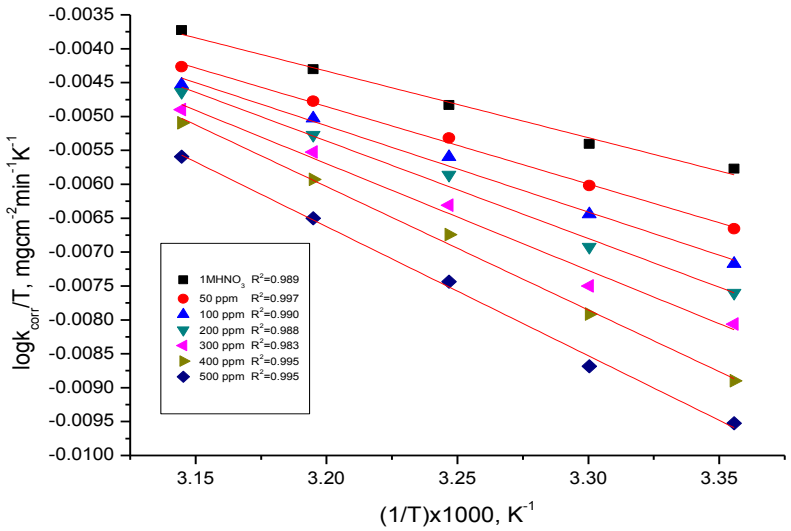

Figure 9: log k (corrosion rate) /T – 1/T curves for copper in 1 M HNO_3in the absence and presence of different concentrations of HME.

Table 6: Activation parameters for dissolution of copper in the absence and presence of different concentrations of HME in 1 M HNO_3.

Conc. ppm	E_a^*, kJ mol^{-1}	ΔH^*, J mol^{-1}	$-\Delta S^*$, J $mol^{-1}K^{-1}$
1.0 M HNO_3	54.27	81.64	197.05
50 ppm	55.34	94.94	196.96
100 ppm	65.20	105.75	196.89
200 ppm	66.51	119.55	196.79
300 ppm	71.80	130.86	196.72
400 ppm	80.26	151.31	196.57
500 ppm	94.12	158.38	196.53

3.7. Surface analysis by SEM

Fig.10 shows an SEM photograph recorded for copper samples Polished (A) and exposed for 12 h in 1M HNO_3 solution without (B) and with 500 ppm of HME at $25C^0$. A photograph of the polished copper surface before immersion in 1 M HNO_3 solution is shown in Fig. 10a. The photograph shows the surface was smooth and without pits. The SEM micrographs of the corroded copper in the presence of 1 M HNO_3 solution are shown in Fig. 10b. The faceting seen in this figures was a result of pits formed due to the exposure of copper to the acid. The influence of the inhibitor addition 500 ppm on the copper in 1 M HNO_3 solution is shown in Fig. 10c. The morphology in Fig. 10c shows a rough surface, characteristic of uniform corrosion of copper in acid, as previously reported [50], that corrosion does not occur in presence of inhibitor and hence corrosion was inhibited strongly when the inhibitor was present in the nitric acid, and the surface layer is very rough. In contrast, in the presence of 500 ppm of HME, there is much less damage on the copper surface, which further confirm the inhibition action. Also, there is an adsorbed film adsorbed on copper surface (Fig. 10c). In accordance, it might be concluded that the adsorption film can efficiently inhibits the corrosion of copper.

3.8. Mechanism of the corrosion inhibition

The adsorption of organic compounds can be described by two main types of interactions: physical adsorption and chemisorption. In general, physical adsorption requires the presence of both the electrically charged surface of the metal and charged species in solution. The surface charge of the metal is due to the electric field existing at the metal/solution interface. A chemisorption process, on the other hand, involves charge sharing or charge transfer from the inhibitor molecules to the metal surface to form a coordinate type of a bond. This is possible in

case of a positive as well as a negative charge of the surface. The presence of a transition metal, having vacant, low-energy electron orbitals (Cu^{+} and Cu^{+2})and an inhibitor with molecules having relatively loosely bound electrons or heteroatoms with a lone pair of electrons is necessary for the inhibiting action [51].

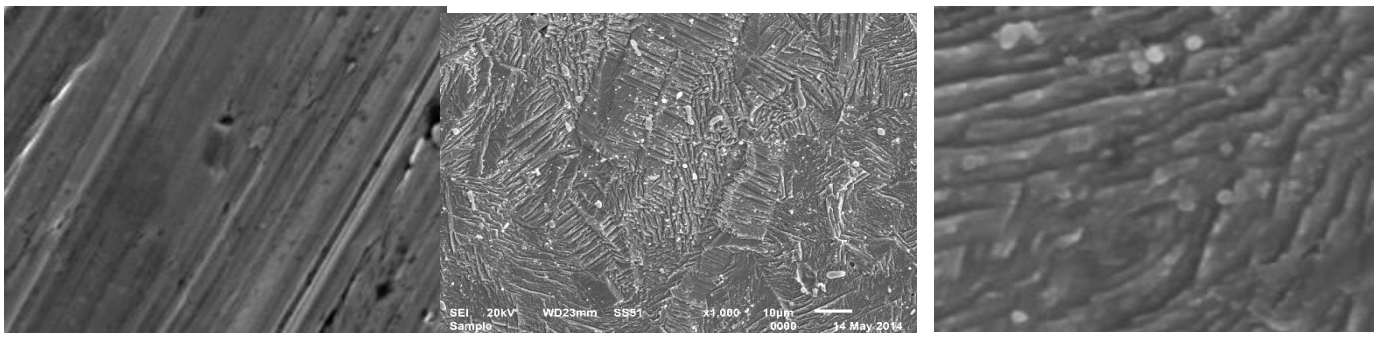

(a) **(b)** **(C)**

Figure 10: SEM micrographs of copper surface (a) before of immersion in 1 M HNO_3, (b) after 12 h of immersion in 1 M $HNO_3$and (c) after 12 h of immersion in 1 M HNO_3 + 500 ppm of HME at 25°C.

Generally, two types of mechanisms of inhibition were proposed. One was the formation of polymeric complexes with copper ions (Cu^{+} and Cu^{+2})depending on the applied conditions [52, 53]. The other was the chemical adsorption of HME on copper surfaces [54, 55]. The inhibition action of HME does not occur by the simple blocking at the surface of copper, especially at high temperature. This might be attributed to the different adsorption capacities of the anise extract on the copper surface at different temperatures. It has been studied that with the increase in temperature, the desorption effect of HME on copper surface decreased. Some of the hydrophilic groups with positively charged atoms (O^{+}) desorbed from the surface of copper and did more work to prevent the H^{+} from getting nearer to the metal surface. Therefore, HME preferentially inhibited the cathodic corrosion process at high temperature.

Conclusions

From the overall experimental results the following conclusions can be deduced:
1. The HME shows good performance as corrosion inhibitor in 1 M HNO_3.
2. The results obtained from weight loss showed that the inhibiting action increases with the HME concentration and decreases with the increasing in temperature.
3. Double layer capacitances decrease with respect to blank solution when the plant extract is added. This fact confirms the adsorption of plant extract molecules on the copper surface.
4. The HME inhibits the corrosion by getting adsorbed on the metal surface following Langmuir adsorption isotherm.
5. The inhibition efficiencies determined by weight loss, potentiodynamic polarization and EIS techniques are in reasonably good agreement.

References

1. Trabanelli G., *Corrosion*, 47 (1991) 410.
2. Singh D. N., Dey A. K., *Corrosion*, 49 (1993) 594.
3. Banerjee G., Malhotra S. N., *Corrosion*, 48 (1992) 10.
4. Arab S. T., Noor E. A., *Corrosion*, 49 (1993) 122.
5. Raspini I. A.,*Corrosion*, 49 (1993) 821.
6. Khadraoui A., Khelifa A., Touafri L., Hamitouche H., Mehdaoui R., *J. Mater. Environ. Sci.* 4 (2013) 663.
7. Elachouri M., Hajji M. S., Salem M., Kertit S., Coudert R., Essassi. E. M., *Corros. Sci.*, 37 (1995) 381.
8. Kertit S., Hammouti B., *App. Surf. Sci.*, 93 (1996) 59.
9. Migahed M. A., Azzam E. M. S., Al-Sabagh A. M., *Mater. Chem.Phys*, 85 (2004) 273.
10. Villamil R. F. V., Corio P., Rubim J. C., Siliva Agostinho M. L., *J. Electroanal. Chem.*, 472 (1999) 112.
11. Hari Kumar and S. Karthikeyan., *J. Mater. Environ. Sci.* 3 (5) (2012) 925–934.
12. Hadi Z.M. Al-Sawaad, Alaa S.K. Al-Mubarak, Athir M. HaddadI., *J. Mater. Environ. Sci.* 1 (4) (2010) 227-238.
13. Abd El Rehim S. S., Hassan H., Amin M. A., *Mater. Chem. Phys.*, 78 (2003) 337.
14. Guo R., Liu T., Wei X., *Colloids Surf, A*, 209 (2002) 37.

15. Branzoi V., Golgovici F., Branzoi F., *Mater.Chem.Phys*, 78 (2002) 122.
16. Parikh K. S., Joshi K. J., *Trans. SAEST*, 39 (2004) 29.
17. Chauhan J. S., *Asian Journal of Chemistry*, 21 (2009) 1975.
18. Sangeetha T. V., Fredimoses M., *E-Journal of Chemistry*, 8 (2011) (S1), S1-S6.
19. Fernando Sílvio de Souza, Cristiano Giacomelli, Reinaldo Simões Gonçalves, Almir Spinelli, *Materials Science and Engineering*, 32 (2012) 2436.
20. Abd-El-Nabey B. A., Abdel-Gaber A. M., El. Said Ali M., Khamis E., El-Housseiny S., *J. Electrochem. Sci*., 8 (2013) 5851.
21. El Sheikh M. O. A., El Hassan G. M., El Tayeb A. H., Abdallah A. A., Antoun M. D., 1982. Studies on Sudanese medicinal plants III: indigenous Hyoscyamus muticus as possible commercial source for hyoscyamine. Planta Medica 45: 116–119.
22. Eeva M., Salo J. P., Oksman-Caldentey K. M., *J. Pharm Biomed Anal*. 1998; 16(5):717. "Determination of the main tropane alkaloids from transformed Hyoscyamus muticus plants by capillary zone electrophoresis".
23. Mu G. N., Zhao T. P., Liu M., Gu T., *Corrosion*, 52 (1996) 853.
24. Parr R. G., Donnelly R. A., Levy M. Palke W. E., *J. Chem. Phys*., 68(1978) 3801.
25. Bosch R. W., Hubrecht J., Bogaerts W. F., Syrett B. C., *Corrosion*, 57(2001) 60.
26. Zhang D. Q.,Cai Q. R.,He X. M., Gao L. X.,Kim G. S., *Mater. Chem. Phys*. 114 (2009) 612.
27. Lee H. P., Nobe K., *J. Electrochem. Soc*. 133 (1986) 2035.
28. Tao Z. H., Zhang S. T., Li W. H., Hou B. R., *Corros. Sci*.51 (2009) 2588.
29. Ferreira E. S., Giacomelli C., Giacomelli, F. C., Spinelli A., *Mater. Chem.Phys*.83 (2004) 129.
30. Paskossy T., *J. Electroanal. Chem*, 364 (1994) 111.
31. Growcock F. B., Jasinski J. H., *J. Electrochem. Soc*., 136 (1989) 2310.
32. Abd El-Rehim S. S., Khaled K. F.,Abd El-Shafi N. S., *Electrochim. Acta*, 51 (2006) 3269.
33. Metikos M., Hukovic R., Bobic Z. Gwabac S., *J. Appl. Elactrochem*., 24 (1994) 772.
34. Caprani A., Epelboin I., Morel Ph., Takenouti H., *Proceedings of the 4th European sym. on Corros. Inhibitors*, (1975) 571.
35. Bessone J., Mayer C., Tuttner K., Lorenz W. J., *Electrochim. Acta*, 28 (1983) 171.
36. Epelboin I., Keddam M., Takenouti H., *J. Appl. Electrochem*., 2 (1972) 71.
37. Benedeti A. V.,Sumodjo P. T. A., Nobe K., Cabot P. L., Proud W. G., *Electrochimica Acta*, 40 (1995) 2657.
38. Ma H., Chen S., Niu L., Zhao S., Li S., Li D., *J. Appl. Electrochem.* 32 (2002) 65.
39. Li X. H.,Deng S. D., Fu H., *J. Appl. Electrochem*., 40 (2010) 1641.
40. Lagrenee M., Mernari B., Bouanis M., Traisnel M., Bentiss F., *Corros. Sci*., 44 (2002) 573.
41. Kus E., Mansfeld F., *Corros. Sci*., 48 (2006) 965.
42. Caigman G. A., Metcalf S. K., Holt E. M., *J.Chem. Cryst*, 30 (2000) 415.
43. Abdel–Rehim S. S., Khaled K. F., Abd–Elshafi N. S., *Electrochim. Acta*, 51 (2006) 3269.
44. Bockris J. O., Swinkels D. A. J., *J. Electrochem. Soc*., 111 (1964)736.
45. Saleh M. M., Atia A. A., *J. Appl. Electrochem*., 36 (2006) 899.
46. Narvez L., Cano E., Bastidas D. M., *J. Appl. Electrochem*., 35 (2005) 499.
47. Li X. H., Deng S. D., Fu H., *Corros. Sci*., 51 (2009) 1344.
48. Putilova I. K., Balezin S. A., Barasanik Y. P., *Metallic Corrosion Inhibitors, Oxford: Pergamon Press*, (1960) 30.
49. Saliyan V. R., Adhikari A. V., *Bull. Mater. Sci*., 31 (2007) 699.
50. Li Y., Zhao P., Liang Q., Hou B., *Appl. Surf. Sci*., 252 (2005) 1245.
51. Mehaute A. H., Grepy G., *Solid State Ionics*, 9–10 (1989) 17.
52. Brusic V., Frisch M. A., Eldridge B. N., Novak F. P., Kauman F. B., Rush B. M., Frankel G. S., *J. Electrochem. Soc*. 138 (1991) 2253.
53. Antonijevic M. M., Petrovic M. B., *Int. J. Electrochem. Sci*.3 (2008) 1.
54. Musiani M. M., Mengoli G., *J. Electroanal. Chem*. 217 (1987) 187.
55. Lewis G., *Corrosion* 34 (1978) 424.